Development of a multiparametric ultrasound image using an integrated system and method to assess hepatic steatosis

Lokesh Basavarajappa [1], Mawia Khairalseed [2,3], Kevin J. Parker [4], Kenneth Hoyt [2,3]

[1] Department of Bioscience and Biomedical Engineering, Indian Institute of Technology Indore, Madhya Pradesh, India
[2] Department of Biomedical Engineering, Texas A&M University, College Station, TX, USA
[3] Department of Small Animal Clinical Sciences, Texas A&M University, College Station, TX, USA
[4] Department of Electrical and Computer Engineering, University of Rochester, Rochester, NY, USA

2024 IEEE South Asian Ultrasonics Symposium (SAUS) | 979-8-3503-8401-7/24/$31.00 ©2024 IEEE | DOI: 10.1109/SAUS61785.2024.10563849

***Abstract*—Nonalcoholic fatty liver disease (NAFLD) is the most common cause of liver disease that includes a progression from steatosis, nonalcoholic steatohepatitis (NASH), to cirrhosis. Currently, liver biopsy is the gold standard for identifying the histologic characteristics of NAFLD; nevertheless, its use is restricted due to its invasiveness, sample inaccuracy, and other hazards. There is an ongoing clinical need for the ability to detect, accurately stage, and reliably monitor NAFLD noninvasively. We have recently presented an *in vivo* multiparametric ultrasound (mpUS) imaging method for the evaluation of NAFLD. The mpUS imaging combines contrast-enhanced ultrasound (CEUS), shear wave elastography (SWE), and H-scan ultrasound (US) measurements. In this study, we developed a mpUS map for the detection of early liver steatosis. Using Sprague-Dawley rats fed either standard control chow ($N = 8$) or a methionine and choline deficient (MCD) diet ($N = 12$) that is known to induce liver steatosis, mpUS imaging was performed at baseline and again at 2 wk. After the animals were euthanized, the livers were removed for *ex vivo* examination. The MCD diet fed animals showed statistically significant differences ($p < 0.05$) in their mean mpUS map data between baseline and two weeks. These results were confirmed by histological findings showing that rats given the MCD diet had liver steatosis.**

Keywords — contrast-enhanced ultrasound, fatty liver disease, H-scan ultrasound, shear wave elastography, multiparametric ultrasound map.

I. Introduction

Nonalcoholic fatty liver disease (NAFLD) is the most common cause of liver disease that affects around 42% of the Southeast Asian population [1]. The increasing incidence of diabetes, metabolic syndrome, hypertension, and obesity have a substantial influence on NAFLD. This group of diseases includes a broad spectrum of histopathological conditions including early-stage steatosis, nonalcoholic steatohepatitis (NASH), and late-stage cirrhosis. Differentiating between steatosis and NASH is crucial for the management of NAFLD patients since it is expected that NASH-induced cirrhosis will eventually become the most common reason for liver transplantation [2]. If steatosis is identified early, individuals can take precautions to prevent it from becoming a more serious condition.

Some researchers have suggested that a liver biopsy may be necessary for all NAFLD patients [3]. Liver biopsies are invasive and know to be associated with sample inaccuracies, inter- and intra-rater variability, poor patient acceptability, and possible side effects such as hemorrhage and sometimes death [4]. In contrast, a significant amount of work has been devoted to the development of noninvasive imaging methods that can accurately detect and stage NAFLD. Ideally, the findings of these imaging methods could be used as a biomarker to reduce or eliminate the need for invasive liver biopsies.

Magnetic resonance imaging-derived proton density fat fraction (MRI-PDFF) measures can accurately detect steatosis via quantification of liver fat content [5]. However, it is not a realistic option for routine clinical screening of patients suspected of having NAFLD. Alternatively, ultrasound (US) imaging is evolving as a promising and cost-effective solution for the early detection of steatosis [6]. To that end, our research group has developed multiparametric US imaging approaches for the assessment of NAFLD and have evaluated performance with a series of preclinical [7], [8], [9] and clinical [10], [11], [12] studies. Using a rat model of NAFLD, fat quantification using a combination of US parameters outperformed MRI-PDFF for the early detection of liver steatosis [13]. One mpUS approach under investigation integrates tissue viscoelasticity estimates obtained by shear wave elastography (SWE), assessment of hepatic tissue perfusion using contrast-enhanced US (CEUS), and measures of relative scatterer size from the H-scan US tissue characterization method. Each of these US imaging modes provides complementary information and unique insight into select characteristics of NAFLD. In this present study, we introduce an integrated mpUS imaging system and method that performs data acquisition along a single image plane to create a mpUS spatial map from co-registered tissue measurements. This mpUS map was reconstructed using a combination of individually weighted mpUS parameters.

II. Methods and Materials

A. Animal Preparation

All animal experiments were approved by an Institutional Animal Care and Use Committee (IACUC). Sprague-Dawley rats (Charles River Laboratories, Wilmington, MA) were randomly divided into two groups, namely, control ($N = 8$) and diet ($N = 12$). Diet animals received a special methionine and choline deficient (MCD) chow that is known to cause NAFLD, whereas control animals were provided standard food. Rats were anesthetized using 1 to 2% isoflurane and positioned on a temperature-controlled heating pad to maintain core levels throughout all experiments.

B. Liver Measurements

Animals were prepared for *in vivo* mpUS imaging using clippers and depilation cream to shave the abdominal surface. A catheter was then placed and secured in the tail vein to administer a microbubble (MB) contrast agent as needed for

CEUS imaging. The US transducer was appropriately positioned in the transverse plane of each animal to avoid major blood vessels. Effort was made to find the same imaging plane in each animal during subsequent sessions. mpUS imaging was implemented on a programmable US system (Vantage 256, Verasonics Inc, Kirkland, WA) equipped with an L11-4v linear array transducer. Liver imaging was performed at baseline (0 week) and again after 2 weeks of feeding with standard (control) or MCD chow (diet). The entire mpUS image acquisition procedure typically lasted less than 5 min. All US data was saved for offline processing using custom MATLAB software (MathWorks, Natick, MA). A common region-of-interest (ROI) was selected for each liver and used for all mpUS parametric measurements.

C. mpUS Parameters

The system and method used for generating H-scan US images was detailed previously [14], [15]. Briefly, raw radiofrequency (RF) data was acquired and processed using a pair of convolutional filters constructed using Gaussian-weighted Hermite polynomial functions of order 2 and 8 (denoted GH_2 and GH_8, respectively). The relative strength of these filter outputs was normalized by the signal energy $\sqrt{E_n}$. The lower frequency backscattered US signals (GH_2) were then assigned to a red (R) channel and higher frequency components (GH_8) to a blue (B) channel. The envelope of the original unfiltered data was assigned to a green (G) channel to complete the RGB color map. H-scan US image intensity I_H was distributed using the well-known luminosity weighted average method as follows:

$$I_H = 0.299 \times R + 0.587 \times G + 0.114 \times B \qquad (1)$$

SWE functionality was implemented using 3 long and rapid push pulse sequences applied using a pulse frequency of 5.2 MHz, aperture size of 64 elements, pulse length of 230 μs, and axial spacing between push beams of 2 mm [7]. After the induction of shear waves, ultrafast plane wave imaging with a frame rate of 10 kHz was used to track propagation across an area of interest. Tissue displacements were estimated from the beamformed in-phase quadrature (IQ) data using the Loupas algorithm [16]. A 2-dimensional (2D) fast Fourier transform of the processed tissue displacements was used to estimate liver tissue viscoelasticity parameters like the shear wave speed (SWS) and shear wave attenuation (SWA) [17].

CEUS imaging was performed using an amplitude modulated contrast pulse sequence that combines backscattered US signals from two half-amplitude pulses and a full-amplitude pulse transmissions [18]. After bolus injection of MBs (50 μL; Definity, Lantheus Medical Imaging, N Billerica, MA) via a tail vein catheter, a sequence of CEUS images was acquired for approximately 30 sec. This data was then combined and processed for additional tissue suppression using singular value decomposition (SVD) filtering [19]. The mean time intensity curve was constructed for each ROI from the liver parenchyma. From this curve, tissue perfusion parameters like peak enhancement (PE) and wash-in rate (WIR) were calculated [20].

D. mpUS Image Reconstruction

The final mpUS map was generated from six different US parametric measurements. Following Z-score normalization

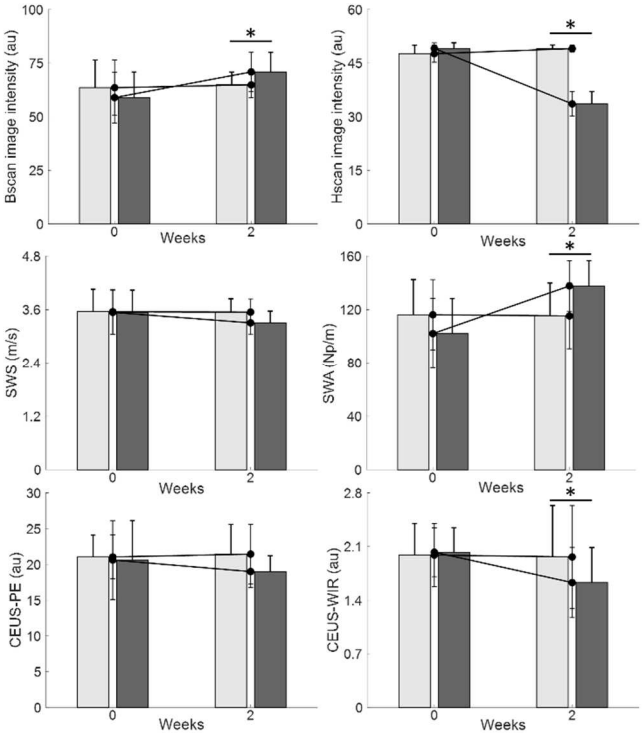

Fig. 1. Summary of multiparametric ultrasound (mpUS) parameters at baseline and 2 wks after animals were fed standard (control, light gray) or chow known to induce liver steatosis (diet, dark gray). Abbreviations: SWS, shear wave speed; SWA, shear wave attenuation; CEUS-PE, contrast-enhanced ultrasound peak enhancement; CEUS-WIR, contrast-enhanced ultrasound wash-in rate.

for each mpUS parameter, a linear support vector machine (SVM) model was trained using the normalized values. The weights w_i from each mpUS parameter were estimated and then applied to the US image intensity I_i for that parameter before combining to form the final mpUS image intensity I_{mpUS}. This process can be represented as follows:

$$I_{mpUS} = \sum_{i=1}^{6} w_i \times I_i \qquad (2)$$

E. Histology

After two weeks of mpUS imaging, animals were humanely euthanized and livers were surgically excised for histological assessment. Liver tissue samples were embedded in paraffin, sectioned (5 μm), and stained with hematoxylin and eosin (H&E). Digital images of each tissue section were acquired using an optical microscope (Axio Observer 7, Carl Zeiss, Thornwood, NY). The percentage of liver fat from the H&E images was calculated using an established method [7].

F. Performance Measures

Experimental data was summarized as mean ± standard deviation. A Mann-Whitney U test was used to assess differences between control and diet group datasets from US and histological analyses. A p-value less than 0.05 was considered statistically significant. All statistical analyses were performed using Prism 9 (GraphPad Software Inc, San Diego, CA).

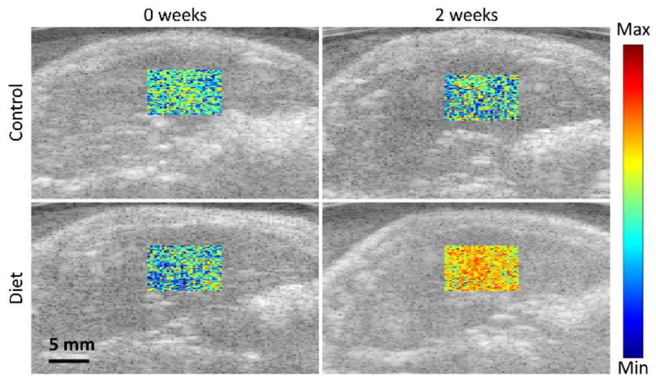

Fig. 2. Representative mpUS map overlaid on the B-scan ultrasound (US) images for anatomical guidance. A weighted combination of six different US parameters contributes to the local mpUS image intensity.

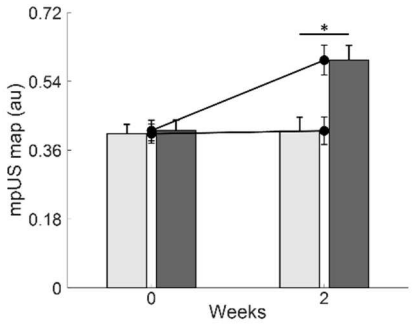

Fig. 3. Plot of mpUS image intensity at 0 and 2 wks from animals fed a control (light gray) or MCD (dark gray) diet known to induce liver steatosis.

III. Results

A summary of individual US measurements is detailed in Fig. 1. While we found no changes in control animal measures, there were significant differences in the B-scan, H-scan, SWA, and CEUS-WIR parameters after 2 wks of feeding animals an MCD diet ($p < 0.05$). Using these individual US measures, a single mpUS image was generated after appropriate value scaling and weighting using eqn. (2). Representative mpUS images from control and diet animals at baseline and after 2 wks of feeding are presented in Fig. 2. The SVM weights used to combine the various US image-derived parameters are summarized in Table I. From inspection of Fig. 2, it can be inferred that while there is no change in the mpUS images from the control animals, there is pronounced change in the mpUS images from the MCD diet fed animals at 2 wks. A summary plot of mean mpUS parameter is shown in Fig. 3. While baseline measurements were comparable, mpUS images exhibited significant differences after only 2 wks of animals being fed a normal or MCD diet ($p < 0.05$).

Table I: Summary of the support vector machine (SVM) weights derived from analysis of the various US image-derived parameters and then used to reconstruct the final mpUS images. Abbreviations: SWS, shear wave speed; SWA, shear wave attenuation; CEUS-PE, contrast-enhanced ultrasound peak enhancement; CEUS-WIR, contrast-enhanced ultrasound wash-in rate.

B-scan	H-scan	SWS	SWA	CEUS-PE	CEUS-WIR
−0.022	−1.23	0.11	−0.09	−0.39	−0.14

After the final US imaging session at 2 wks, animals were euthanized, and livers were surgically excised for histological processing. Representative histology images of liver tissue from a control and MCD diet group animal are shown in Fig. 4. Inspection of these images reveal that the MCD diet fed animal had a considerate amount of liver steatosis. The corresponding mean liver fat fraction from the control and diet and control group animals was found to be $0.73 \pm 0.13\%$ and $17.0 \pm 1.42\%$, respectively ($p < 0.01$).

IV. Discussion

A novel approach for mpUS imaging was introduced. It incorporated complementary parametric information derived from B-scan and H-scan US, SWE, and CEUS imaging. Performance of this mpUS imaging approach was assessed using an animal model of NAFLD. Considering individual US measures, H-scan imaging exhibited the most pronounced changes after feeding animals the MCD diet shown to induce liver stations after only 2 wks. Given the onset of liver steatosis alters the tissue microenvironment and increases the mean distance between neighboring hepatocytes, we hypothesize these changes have a pronounced impact on the backscattered US signals and H-scan analysis of relative scatterer size [21], [22].

Advancements in technology and changes in the healthcare landscape have inspired efforts to broaden the availability of low cost US imaging and integrated mpUS techniques [23]. The mpUS imaging solution detailed herein was inspired in part by research that used linear SVM to combine an ensemble of US parameters for prostate cancer detection [24]. Results from that research demonstrated that mpUS provides enhanced tumor visibility representing a promising technique for targeted transrectal US-guided prostate biopsy. Given the number and clinical value of the

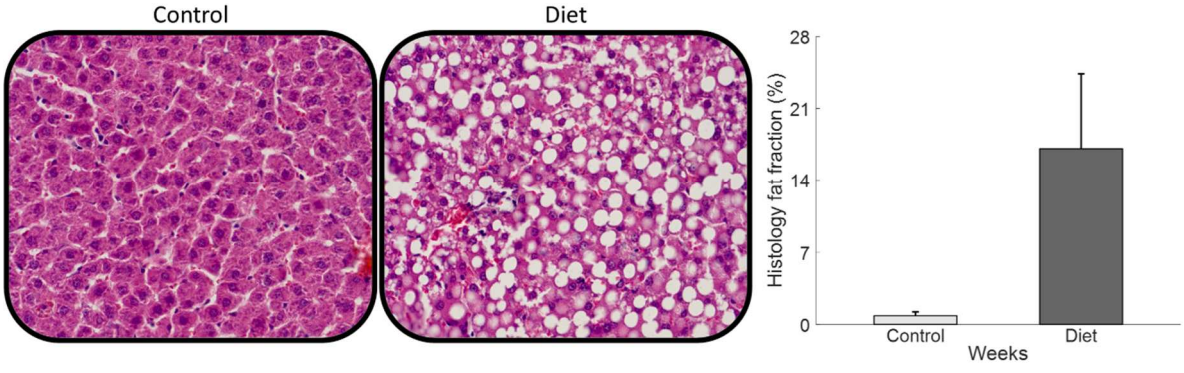

Fig. 4. Representative histology images of liver tissue samples from animals given a control and MCD diet for two weeks are shown with a plot of the corresponding fat fraction values.

different US measures now provided by modern US scanners, a mpUS solution integrating these various parametric measures is increasingly becoming important and has become the focus of ongoing research initiatives [8], [13], [25].

To produce a potentially more impactful mpUS image, future research could incorporate additional US measures that are known to change with NAFLD progression. This approach might allow discrimination of different NAFLD disease stages like NASH from normal and steatotic liver conditions. Preliminary testing should also use animal models that allow selective study of these unique NAFLD conditions.

V. CONCLUSIONS

A novel approach for the mpUS assessment of NAFLD was developed and introduced. Preliminary findings suggest that mpUS imaging has the sensitivity to detect and visualize the early onset and progression of liver steatosis.

REFERENCES

[1] S. Singh, G. N. Kuftinec, and S. Sarkar, "Non-alcoholic fatty liver disease in South Asians: A review of the literature," *J. Clin. Transl. Hepatol.*, vol. 5, no. 1, pp. 76–81, 2017.

[2] R. J. Wong *et al.*, "Nonalcoholic steatohepatitis is the second leading etiology of liver disease among adults awaiting liver transplantation in the United States," *Gastroenterology*, vol. 148, no. 3, pp. 547–555, 2015.

[3] J. K. J. Gaidos, B. E. Hillner, and A. J. Sanyal, "A decision analysis study of the value of a liver biopsy in nonalcoholic steatohepatitis," *Liver Int. Off. J. Int. Assoc. Study Liver*, vol. 28, no. 5, pp. 650–658, 2008.

[4] D. E. Kleiner *et al.*, "Design and validation of a histological scoring system for nonalcoholic fatty liver disease," *Hepatology*, vol. 41, no. 6, pp. 1313–1321, 2005.

[5] B. Wildman-Tobriner *et al.*, "Association between magnetic resonance imaging-proton density fat fraction and liver histology features in patients with nonalcoholic fatty liver disease or nonalcoholic steatohepatitis," *Gastroenterology*, vol. 155, no. 5, pp. 1428–1435, 2018.

[6] A. Ozturk *et al.*, "Quantitative hepatic fat quantification in non-alcoholic fatty liver disease using ultrasound-based techniques: A review of literature and their diagnostic performance," *Ultrasound Med. Biol.*, vol. 44, no. 12, pp. 2461–2475, 2018.

[7] L. Basavarajappa *et al.*, "Multiparametric ultrasound imaging for the assessment of normal versus steatotic livers," *Sci. Rep.*, vol. 11, no. 1, p. 2655, 2021.

[8] J. Baek, L. Basavarajappa, K. Hoyt, and K. J. Parker, "Disease-specific imaging utilizing support vector machine classification of H-scan parameters: Assessment of steatosis in a rat model," *IEEE Trans. Ultrason. Ferroelectr. Freq. Control*, vol. 69, no. 2, pp. 720–731, 2022.

[9] J. Baek *et al.*, "Clusters of ultrasound scattering parameters for the classification of steatotic and normal livers," *Ultrasound Med. Biol.*, vol. 47, no. 10, pp. 3014–3027, 2021.

[10] J. Baek, L. Basavarajappa, A. El Kaffas, A. Kamaya, K. Hoyt, and K. J. Parker, "Multiparametric ultrasound analysis for diagnosis of hepatic steatosis in human subjects," *Proc IEEE Ultrason Symp*, pp. 1–3, 2023.

[11] M. Khairalseed, L. Basavarajappa, A. El Kaffas, A. Kamaya, K. J. Parker, and K. Hoyt, "H-scan ultrasound imaging with adaptive attenuation correction for improved detection of liver steatosis in human subjects," *Proc IEEE Ultrason Symp*, pp. 1–4, 2023.

[12] L. Arthur *et al.*, "Diagnosis of hepatic steatosis using H-scan ultrasound imaging and texture analysis," *Proc IEEE Ultrason Symp*, pp. 1–3, 2023.

[13] J. Baek *et al.*, "Multiparametric ultrasound imaging for early-stage steatosis: Comparison with magnetic resonance imaging-based proton density fat fraction," *Med. Phys.*, vol. 51, no. 2, pp. 1313–1325, 2024.

[14] M. Khairalseed, K. Brown, K. J. Parker, and K. Hoyt, "Real-time H-scan ultrasound imaging using a Verasonics research scanner," *Ultrasonics*, vol. 94, pp. 28–36, 2019.

[15] M. Khairalseed, F. Xiong, J.-W. Kim, R. F. Mattrey, K. J. Parker, and K. Hoyt, "Spatial angular compounding technique for H-scan ultrasound imaging," *Ultrasound Med. Biol.*, vol. 44, no. 1, pp. 267–277, 2018.

[16] T. Loupas, R. B. Peterson, and R. W. Gill, "Experimental evaluation of velocity and power estimation for ultrasound blood flow imaging, by means of a two-dimensional autocorrelation approach," *IEEE Trans. Ultrason. Ferroelectr. Freq. Control*, vol. 42, no. 4, pp. 689–699, 1995.

[17] I. Z. Nenadic *et al.*, "Attenuation measuring ultrasound shearwave elastography and in vivo application in post-transplant liver patients," *Phys. Med. Biol.*, vol. 62, no. 2, pp. 484–500, 2017.

[18] K. Brown and K. Hoyt, "Evaluation of nonlinear contrast pulse sequencing for use in super-resolution ultrasound imaging," *IEEE Trans. Ultrason. Ferroelectr. Freq. Control*, vol. 68, no. 11, pp. 3347–3361, 2021.

[19] D. Ghosh, F. Xiong, S. R. Sirsi, P. W. Shaul, R. F. Mattrey, and K. Hoyt, "Toward optimization of in vivo super-resolution ultrasound imaging using size-selected microbubble contrast agents," *Med. Phys.*, vol. 44, no. 12, pp. 6304–6313, 2017.

[20] R. Saini and K. Hoyt, "Recent developments in dynamic contrast-enhanced ultrasound imaging of tumor angiogenesis," *Imaging Med.*, vol. 6, no. 1, pp. 41–52, 2014.

[21] M. Khairalseed and K. Hoyt, "High-resolution ultrasound characterization of local scattering in cancer tissue," *Ultrasound Med. Biol.*, vol. 49, pp. 951–960, 2023.

[22] M. Khairalseed, K. Hoyt, J. Ormachea, A. Terrazas, and K. J. Parker, "H-scan sensitivity to scattering size," *J. Med. Imaging*, vol. 4, no. 4, p. 043501, 2017.

[23] A. E. Kaffas, J. M. Vo-Phamhi, J. F. Griffin, and K. Hoyt, "Critical advances for democratizing ultrasound diagnostics in human and veterinary medicine," *Annu. Rev. Biomed. Eng.*, vol. 26, pp. 49–65, 2024.

[24] D. C. Morris *et al.*, "Multiparametric ultrasound for targeting prostate cancer: Combining ARFI, SWEI, QUS and B-mode," *Ultrasound Med. Biol.*, vol. 46, no. 12, pp. 3426–3439, 2020.

[25] J. Baek, L. Basavarajappa, K. Hoyt, and K. J. Parker, "Disease specific imaging utilizing support vector machine: Assessment of steatosis," *Proc IEEE Ultrason Symp*, pp. 1–4, 2023.